# PS Late Visean to Bashkirian Platform Cyclicity in the Central Tengiz Buildup (Pricaspian Basin): Depositional Evolution and Reservoir Development*

By

**J.A.M. Kenter[1], P.M. Harris[2], L.J. Weber[3], J.F. Collins[3], M. Stalinski[4], G. Kuanysheva[4], and D.J. Fischer[4]**

Search and Discovery Article #20051 (2008)
Posted May 25, 2008

*Adapted from oral presentation at AAPG Annual Convention, Houston, Texas, April 9-12, 2006

[1]Chevron Energy Technology Company, Amsterdam, Netherlands (jeroenkenter@chevron.com)
[2]Chevron Energy Technology Company, San Ramon, California (MitchHarris@chevron.com)
[3]ExxonMobil Development Company, Houston, Texas
[4]TengizChevroil, Atyrau, Kazakhstan

## Abstract

Cores, logs, and more than 4000 core plugs from four deep wells penetrating upper Viséan-Serpukhovian and Bashkirian supersequences in the central platform portion of the supergiant Tengiz reservoir of western Kazakhstan provide a coherent model of the lithofacies distribution and reservoir development.

Depositional cycles, several to 10’s of meters in thickness, are made up of a succession of lithofacies generally overlying a sharp base with evidence for subaerial exposure. Tight peloidal mudstone and ash beds occur in association with sequence boundaries, reflecting low-energy conditions in deeper platform areas at lowstand and during initial flooding. Beds with brachiopods are shallow low-energy and signal initial open-marine influence. The succeeding crinoid-dominated intervals represent maximum marine flooding, and the overlying skeletal-peloidal to coated grain and ooid/algal grainstone a highstand shoaling phase. Cycles are generally easy to correlate laterally over several km’s distance; identification of the cycle boundaries is indicated by gamma-ray spikes (ash beds).

The present-day distribution of reservoir rock types in the central platform was mostly determined by late burial diagenetic modification of an earlier reservoir system that was controlled by highly cyclic depositional and early diagenetic processes. Late burial diagenesis increased porosity by dissolution and reduced porosity through pyrobitumen cementation. Pyrobitumen increases towards the outer platform and near the base of cycles; this suggests that the first fill of hydrocarbons migrated through the flanks laterally into the platform cycles. Late burial diagenesis “flattened” the initial vertical, nearly cyclic, porosity away from the central platform and generally obscured the relationship between pore types and permeability behavior.

# LATE VISEAN TO BASHKIRIAN PLATFORM CYCLICITY IN THE CENTRAL TENGIZ BUILDUP, PRICASPIAN BASIN, KAZAKHSTAN: DEPOSITIONAL EVOLUTION AND RESERVOIR DEVELOPMENT

**Field Location**

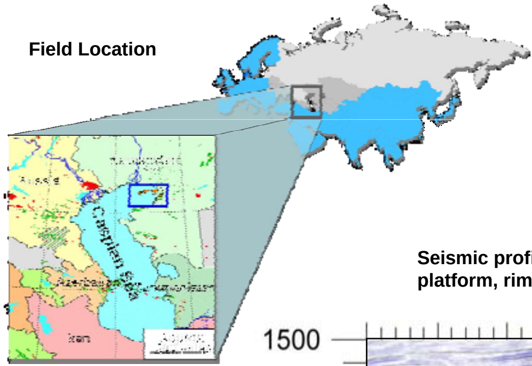

Map of top reservoir (= top Bashkirian), contour interval of 100 m. Line shows location of seismic line below.

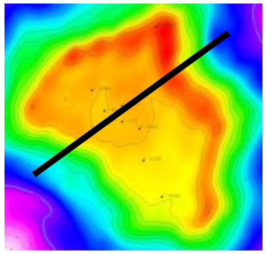

Seismic profile showing general depositional areas (central platform, outer platform, rim-slope or flank) and key reservoir zones (RZ).

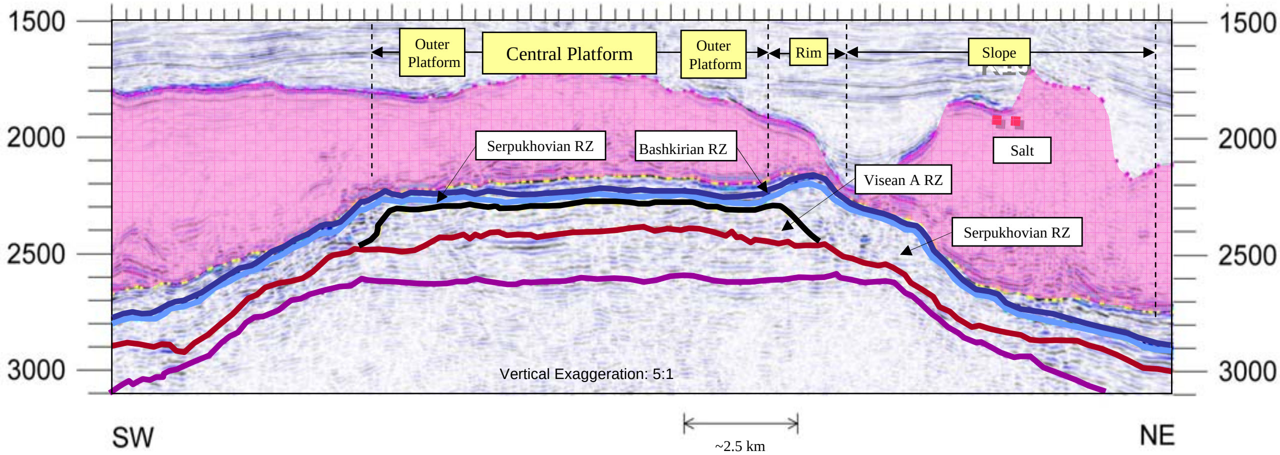


Cross section showing major stratigraphic surfaces and reservoir zonation scheme.

Stratigraphic surfaces, in ascending order, are: Tournaisian (Tour_MFS); Early Visean (Evis_SSB); Late Visean (Lvis1_MFS), (Lvis_SSB), and (Lvis13_csb); Serpukhovian (Serp_SSB); and Bashkirian (Bash_SSB).

Reservoir zones bracketed by these surfaces are: Visean D, Visean C, Visean B, Visean A, Serp, and Bash.

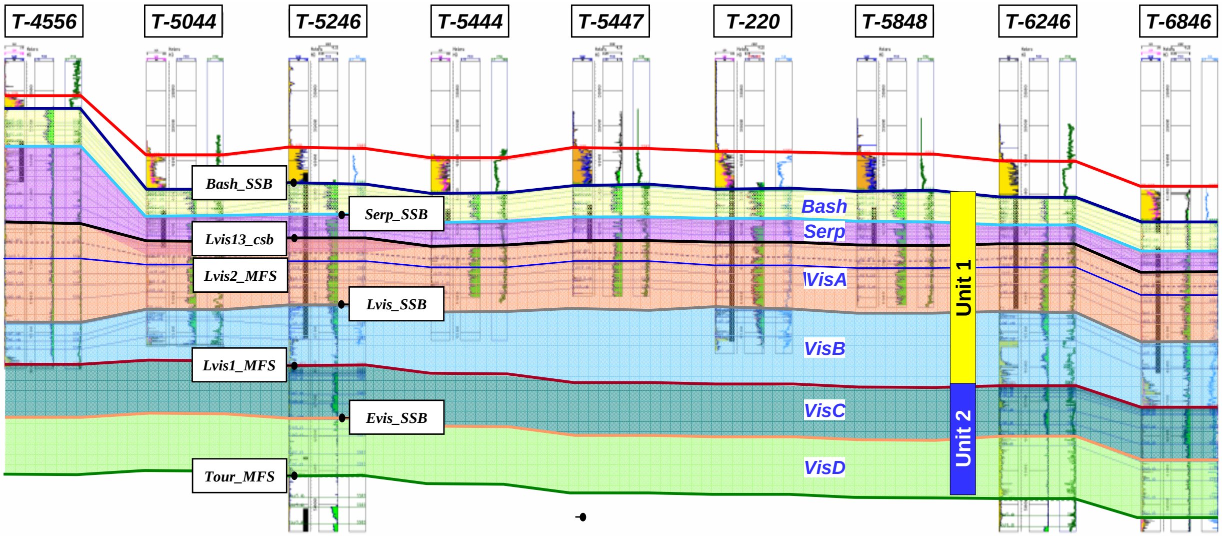


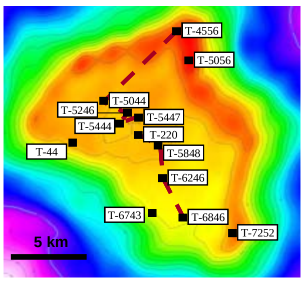

**J. A. M. Kenter** and **P. M. Harris**, Chevron Energy Technology Company

**J. F. Collins** and **L. J. Weber,** ExxonMobil Development Company

**G. Kuanysheva** and **D. J. Fischer**, TengizChevroil

**Cross section show detailed lithofacies and cycle correlations within the central platform region within the Visean A, Serpukhovian, and Bashkirian supersequences. Triangles identify higher order sequences (4th and higher order) correlated from well to well.**

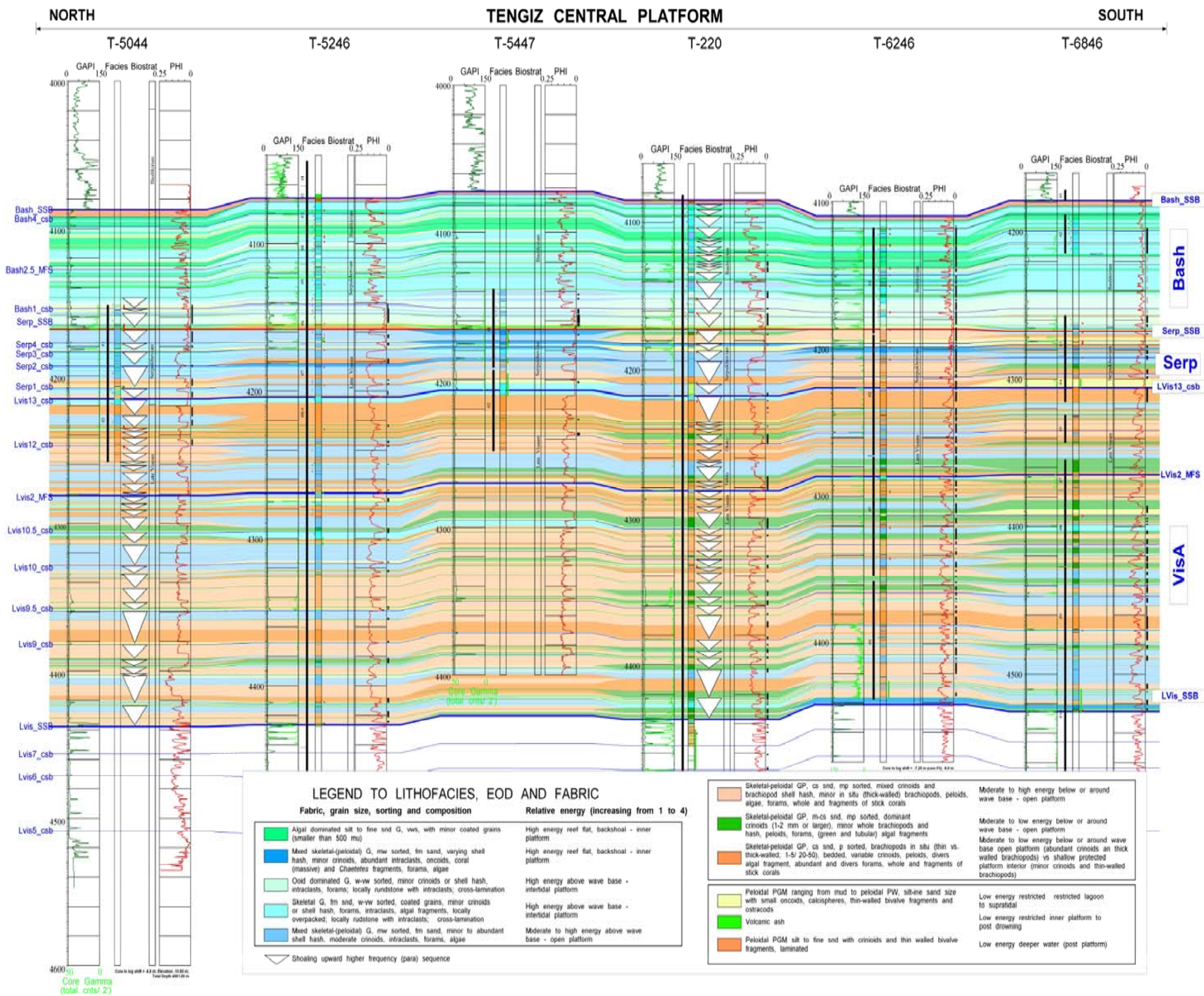

# LATE VISEAN TO BASHKIRIAN PLATFORM CYCLICITY IN THE CENTRAL TENGIZ BUILDUP, PRICASPIAN BASIN, KAZAKHSTAN: DEPOSITIONAL EVOLUTION AND RESERVOIR DEVELOPMENT

| Facies | | EoD |
|---|---|---|
| **Abbreviation** | **General description** | |
| Algal Grainstone (AG) | algal dominated silt to fine snd G, vws, with minor coated grains (smaller than 500 mu) | High energy reef flat, backshoal - inner platform |
| Skeletal Intraclast Grainstone (SIG) | mixed skeletal-(peloidal) G, mw sorted, fm sand, varying shell hash, minor crinoids, abundant intraclasts, oncoids, coral (massive) and *Chaetetes* fragments, forams, algae | High energy reef flat, backshoal - inner platform |
| Coated Grain Grainstone/Rudstone (CgGR) | ooid dominated G, w-vw sorted, minor crinoids or shell hash, intraclasts, forams; locally rundstone with intraclasts; cross-lamination | high energy above wave base - intertidal platform |
| Ooid Grainstone (OG) | skeletal G, fm snd, w-vw sorted, coated grains, minor crinoids or shell hash, forams, intraclasts, algal fragments, locally overpacked; l;ocally rudstone with intraclasts; cross-lamination | high energy above wave base - intertidal platform |
| Well-Sorted Skeletal Grainstone (SPG) | mixed skeletal-(peloidal) G, mw sorted, fm sand, minor to abundant shell hash, moderate crinoids, intraclasts, forams, algae | moderate to high energy above wave base - open platform |
| Poorly Sorted Skeletal-Peloid Grainstone/Packstone (SPP) | skeletal-peloidal GP, cs snd, mp sorted, mixed crinoids and brachiopod shell hash, minor in situ (thick-walled) brachiopods, peloids, algae, forams, whole and fragments of stick corals | moderate to high energy below or around wave base - open platform |
| Crinoid Skeletal-Peloid Grainstone/Packstone (CSP) | skeletal-peloidal GP, m-cs snd, mp sorted, dominant crinoids (1-2 mm or larger), minor whole brachiopods and hash, peloids, forams, (green and tubular) algal fragments | moderate to low energy below or around wave base - open platform |
| Brachiopod Skeletal-Peloid Grainstone/Packstone (BSP) | skeletal-peloidal GP, cs snd, p sorted, brachiopods in situ (thin vs. thick-walled; 1-5/20-50), bedded, variable crinoids, peloids, divers algal fragment, abundant and divers forams, whole and fragments of stick corals | moderate to low energy below or around wave base open platform (abundant crinoids an thick walled brachiopods) vs shallow protected platform interior (minor crinoids and thin-walled brachiopods) |
| Peloid Packstone/Wackestone (PPW) | ranging from mud to peloidal PW, silt-ine sand size with small oncoids, calcispheres, thin-walled bivalve fragments and ostracods | low energy restricted restricted lagoon to supratidal |
| Volcanic ash (VA) | volcanic ash | low energy restricted inner platform to post drowning |

**Models of hypothetical higher-order depositional cycles for the Bashkirian (A) and the Visean A-Serphuhovian (B) showing grain composition and textural trends from the central Tengiz platform through the outer platform and into the flank.**

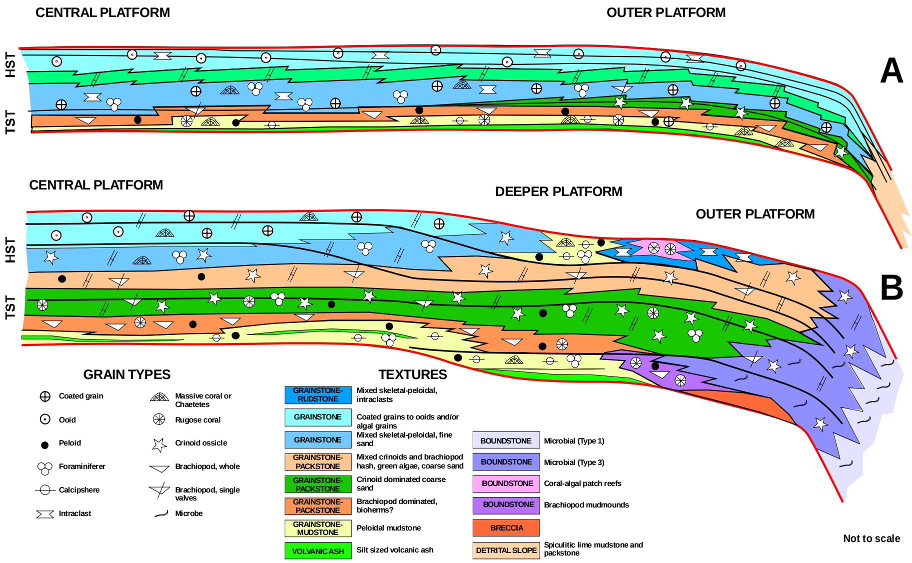


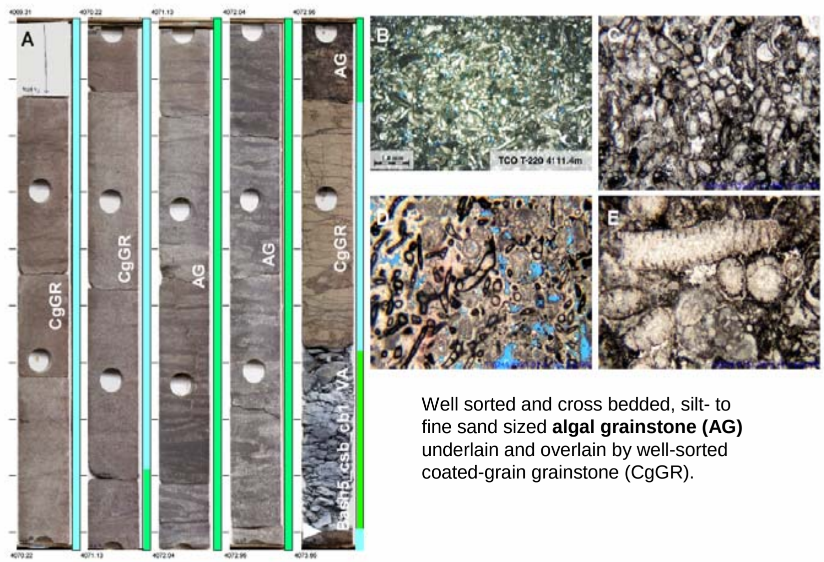


Well sorted and cross bedded, silt- to fine sand sized **algal grainstone (AG)** underlain and overlain by well-sorted coated-grain grainstone (CgGR).

**J. A. M. Kenter** and **P. M. Harris**, Chevron Energy Technology Company

**J. F. Collins** and **L. J. Weber,** ExxonMobil Development Company

**G. Kuanysheva** and **D. J. Fischer**, TengizChevroil

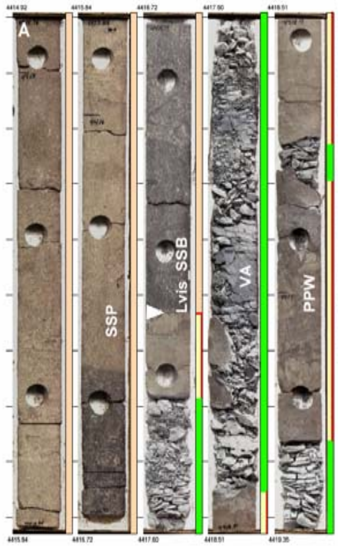


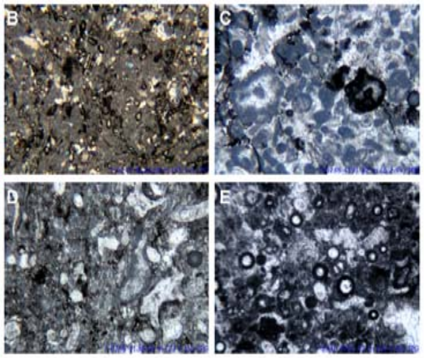


**Peloid packstone/wackestone (PPW)** alternating with volcanic ash layers (VA) below the Lvis_SSB.

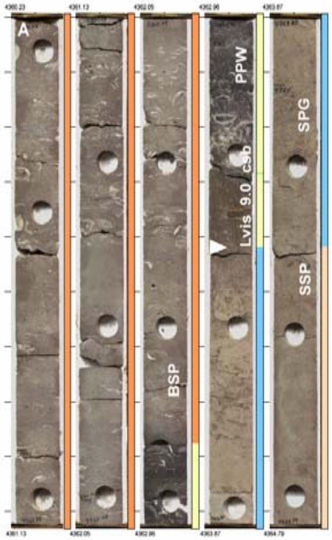


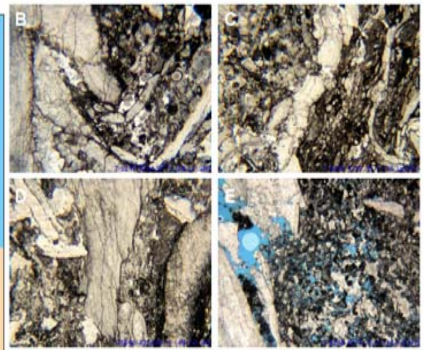


**Skeletal-peloid grainstone-packstone (SSP)** and well-sorted skeletal grainstone (SPG) immediately below the Lvis_9.0_csb.

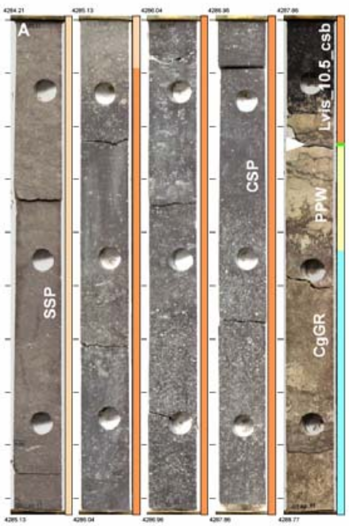


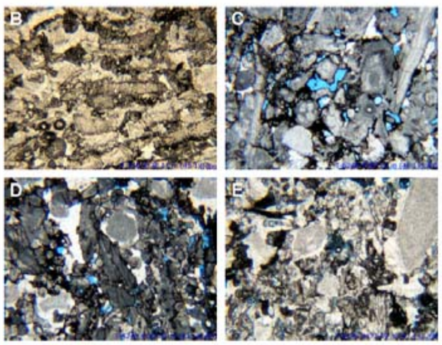


Well-sorted **coated-grain grainstone (CgGR)** overlain by peloid packstone/wackestone (PPW) and capped by the Lvis_10.5_csb.

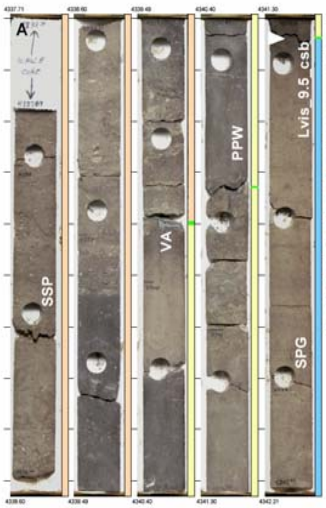


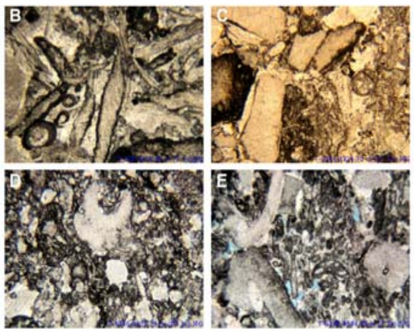


Poorly sorted **skeletal-peloid grainstone-packstone (SPP)** at the top. The lower half of the core contains a shoaling succession of well-sorted skeletal grainstone (SPG) capped by Lvis_9.5_csb.

# LATE VISEAN TO BASHKIRIAN PLATFORM CYCLICITY IN THE CENTRAL TENGIZ BUILDUP, PRICASPIAN BASIN, KAZAKHSTAN: DEPOSITIONAL EVOLUTION AND RESERVOIR DEVELOPMENT

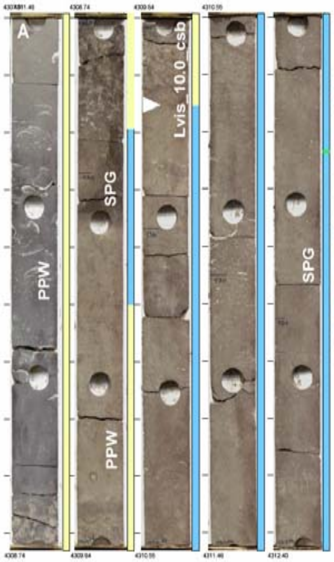


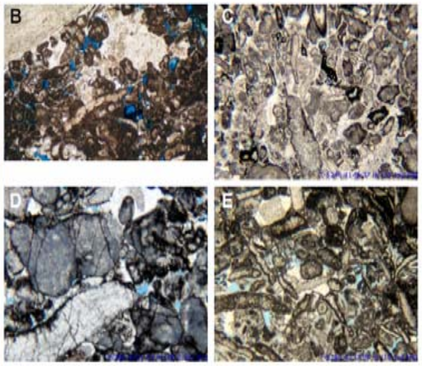


Well-sorted **skeletal grainstone (SPG)** capped by Lvis_10.0_csb.  The boundary is overlain by thin peloid packstone/wackestone (PPW), well-sorted skeletal grainstone (SPG), and peloid packstone/wackestone (PPW).

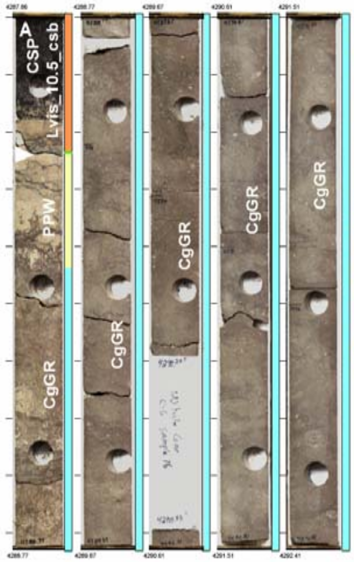


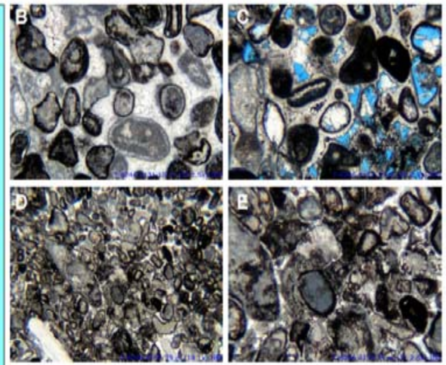


Well-sorted **coated-grain grainstone (CgGR)** overlain by thin peloid packstone/wackestone (PPW). The Lvis_10.5_csb is overlain by coarse, moderately sorted crinoid-dominated skeletal - peloidal sands (CSP).

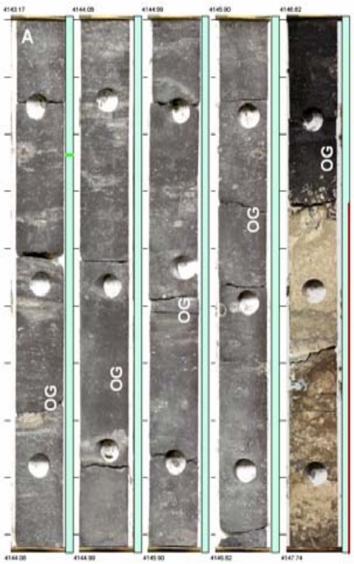


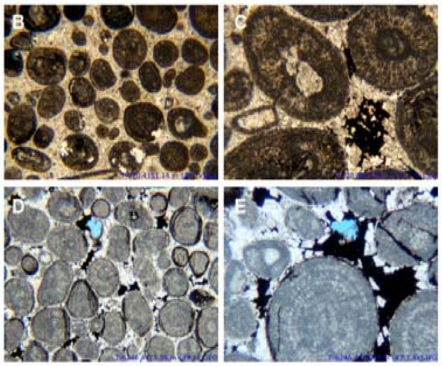


Cross bedded, **well-sorted ooid grainstone (OG).**

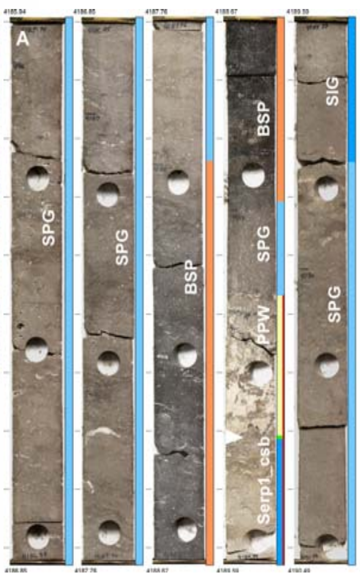


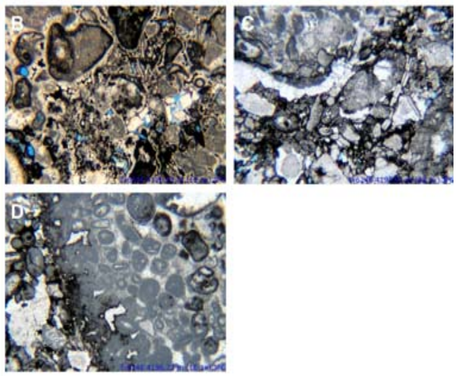


Well-sorted **skeletal grainstone (SPG),** overlain by a relatively thin interval of coarse grained skeletal-intraclast grainstone (SIG), and capped by the Serp1_csb.

# LATE VISEAN TO BASHKIRIAN PLATFORM CYCLICITY IN THE CENTRAL TENGIZ BUILDUP, PRICASPIAN BASIN, KAZAKHSTAN: DEPOSITIONAL EVOLUTION AND RESERVOIR DEVELOPMENT

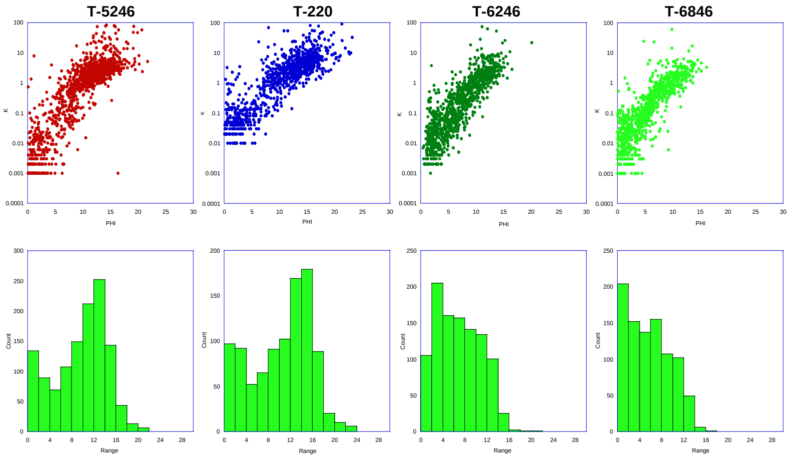


**K-Phi plots (top) and porosity histograms (bottom) suggest different behavior between the northern wells (T-220 and T-5246) and southern wells (T-6246 and T-6846) with generally lower mean porosities and better behaved permeability-porosity relationships in the southern wells and bimodal porosity distributions in the northern wells.**

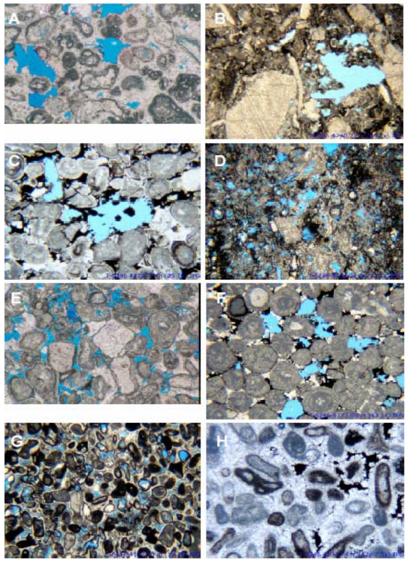

**Vugs shown here are the result of enhanced dissolution in a grainstone following early equant rim cementation.**

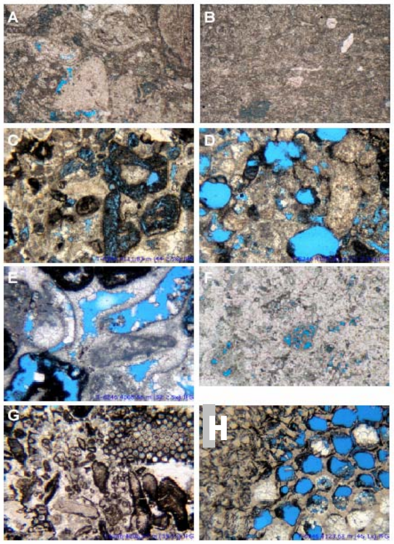

**(A, B) Microporosity developed in grains and matrix; (C-E) Moldic porosity; and (F-H) Intraparticle porosity.**

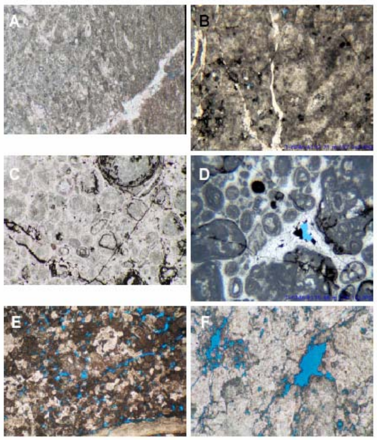

**(A, B) Fractures filled by blocky calcite cement. (C, D) Hairline fissures or fractures filled by bitumen. (E, F) Fractures enhanced by late stage dissolution.**

**Relative contributions by vuggy, intercrystalline and moldic pore types are significantly higher in T-220 for all facies types than in T-6246 which may be related to the larger average grain size and higher contribution by the mud-lean rock types in T-6246. Similarly, cement types in T-6246 show a higher abundance (frequency) of equant calcite and syntaxial cements than in T-220. This may suggest a larger volume of deep burial cements.**

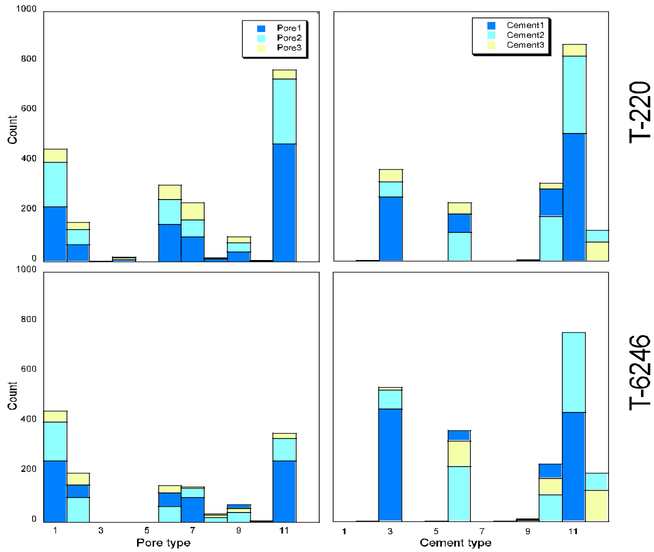


**Pore types are: 1 = interparticle, 2 = intraparticle, 3 = fenestral, 4 = shelter, 5 = growth framework, 6 = intercrystalline, 7 = moldic, 8 = microporosity, 9 = fracture, 10 = channel, 11 = vug, and 12 = enhanced dissolution.**

**Cement types are: 1 = fibrous, 2 = bladed, 3 = equant to rhombic, 4 = coarse crystalline, 5 = botryoidal, 6 = syntaxial, 7 = micritic, 8 = meniscus, 9 = microstalactitic, 10 = poikilotopic, 11 = neomorphic spar, and 12 = grain rims.**

A. M. Kenter and P. M. Harris, Chevron Energy Technology Company
J. F. Collins and L. J. Weber, ExxonMobil Development Company
G. Kuanysheva and D. J. Fischer, TengizChevroil

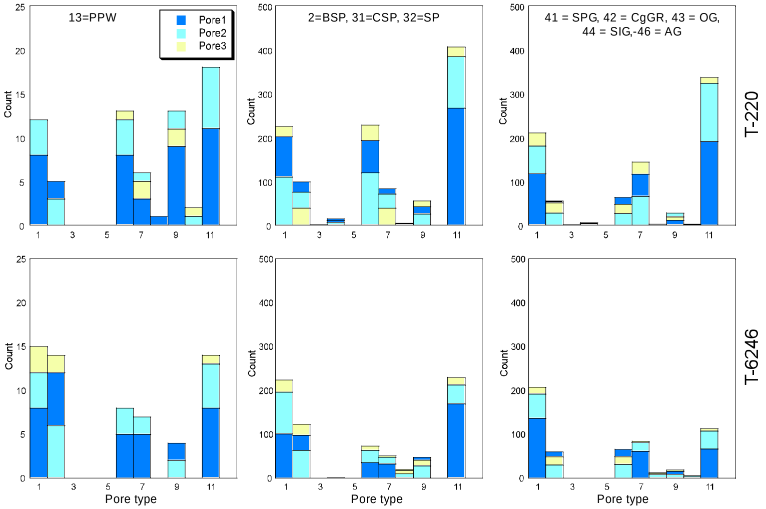


**Pore type contributions for muddy lagoonal facies (13=PPW), moderately sorted grainy facies with mud matrix (2=BSP, 31=CSP, 32=SPP), and mud-lean well sorted grainy facies (41 = SPG, 42 = CgGR, 43 = OG, 44 = SIG,-46 = AG).**

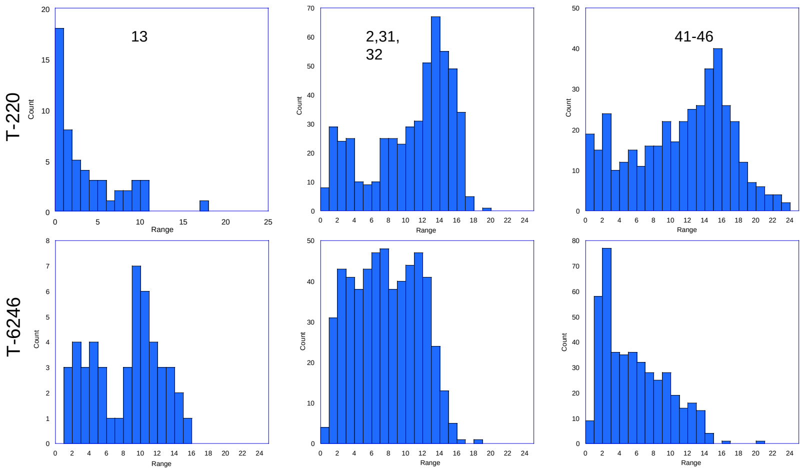


**Porosity distributions for muddy lagoonal facies (13=PPW), moderately sorted grainy facies with mud matrix (2=BSP, 31=CSP, 32=SPP), and mud-lean well sorted grainy facies (41 = SPG, 42 = CgGR, 43 = OG, 44 = SIG,-46 = AG).**

**Bitumen is mostly associated with grainy mud-lean to mud-rich facies (A) and dominantly in interparticle, intercrystalline and vug pore types with minor contributions by intraparticle, moldic and fracture pores (B). Bitumen contents above 0.5 rock volume % shows a negative relationship with porosity (C) and permeability (D).**

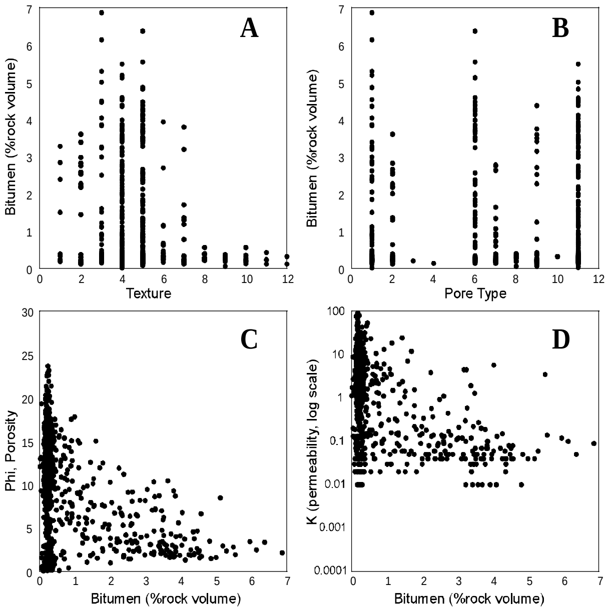


**Pore types are: 1 = interparticle, 2 = intraparticle, 3 = fenestral, 4 = shelter, 5 = growth framework, 6 = intercrystalline, 7 = moldic, 8 = microporosity, 9 = fracture, 10 = channel, 11 = vug, and 12 = enhanced dissolution.**

**Textures are: 1 = rudstone, 2 = grainstone/Rudstone, 3 = grainstone, 4 = grainstone/packstone, 5 = packstone/grainstone, 6 = packstone; 7 = packstone/wackestone, 7 = wackestone/packstone, 8 = wackestone; 9 = wackestone/mudstone, 10 = mudstone/wackestone, 11 = mudstone; and 12 = boundstone.**

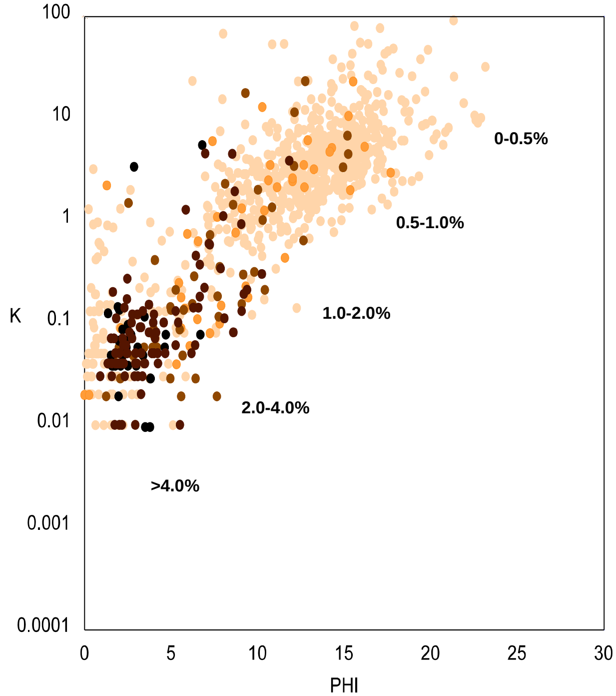


**Increasing bitumen content is negatively correlated with K-Phi above a certain threshold of ~0.5 % rock volume.**

# LATE VISEAN TO BASHKIRIAN PLATFORM CYCLICITY IN THE CENTRAL TENGIZ BUILDUP, PRICASPIAN BASIN, KAZAKHSTAN: DEPOSITIONAL EVOLUTION AND RESERVOIR DEVELOPMENT

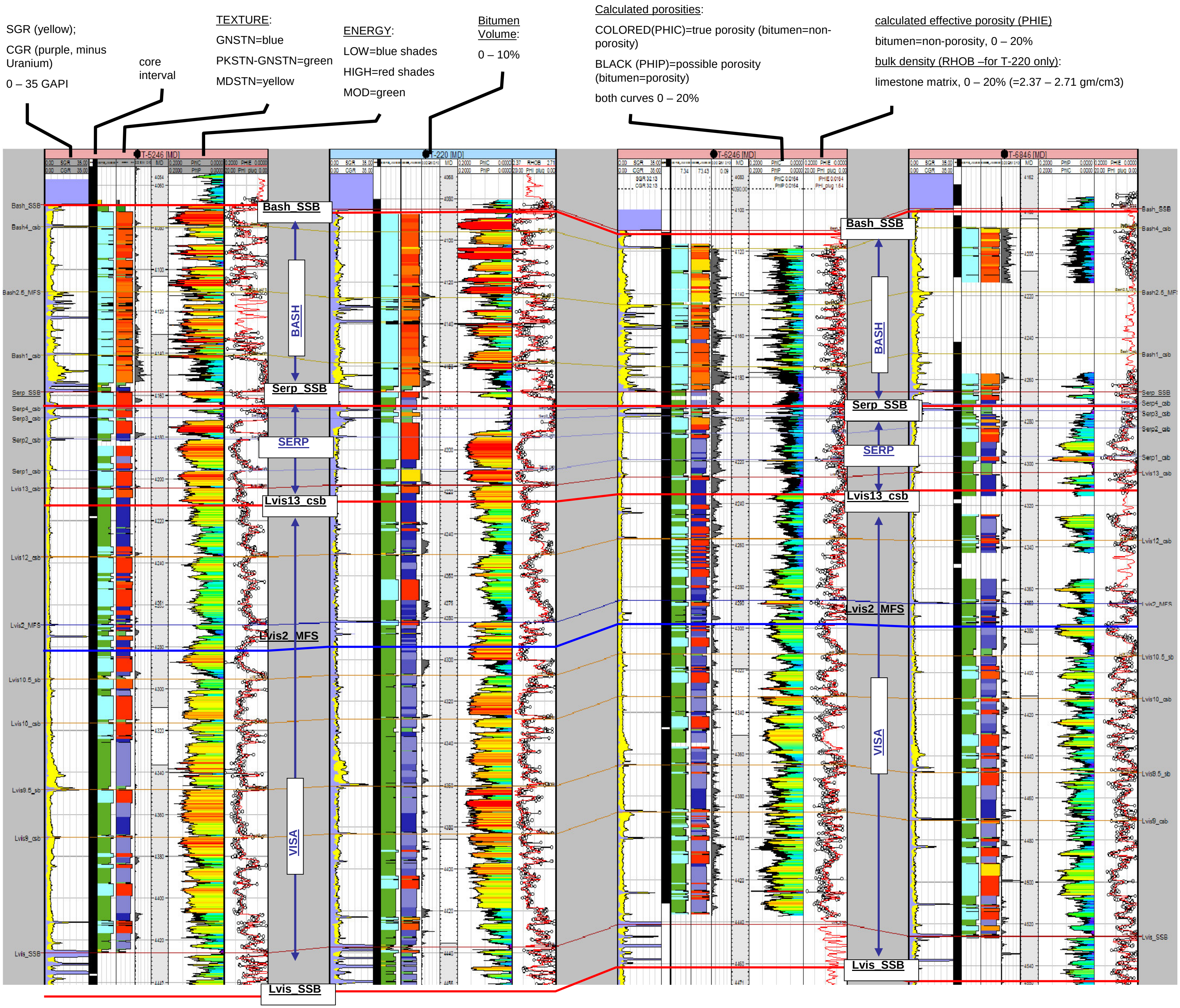


**K-Phi plots and porosity histograms suggest different behavior between northern central platform wells (T-220 and T-5246) and southern central platform wells (T-6246 and T-6846) with generally lower mean porosities and better behaved permeability-porosity relationships in the southern wells and bimodal porosity distributions in the northern wells.**

**J. A. M. Kenter** and **P. M. Harris**, Chevron Energy Technology Company
**J. F. Collins** and **L. J. Weber**, ExxonMobil Development Compar
**G. Kuanysheva** and **D. J. Fischer**, TengizChevroil

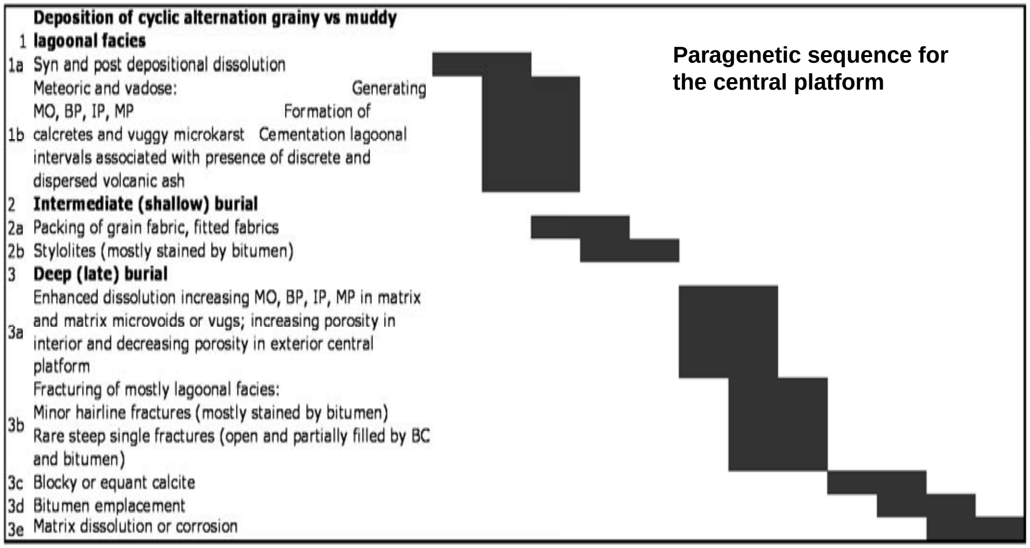


**Porosity creation events**

1b Meteoric and vadose dissolution below PSB and SB

3a Late burial enhanced dissolution affecting BP, MO, MP and MVUG but depending on primary fabric and early pore networks - thereby following primary facies distribution

3e Late burial post bitumen emplacement matrix dissolution or corrosion

**Porosity reduction events**

1 Trapping of volcanic ash in discrete layers and as dispersed agent is associated with elevated cementation calcite and silica) - both in low energy and moderate high energy EoDs and not clear spatial distribution

3c Blocky or equant calcite

3d Emplacement of bitumen related to generation of pore network of contemporanous and/or earlier matrix and fracture dissolution - thereby following primary facies distribution

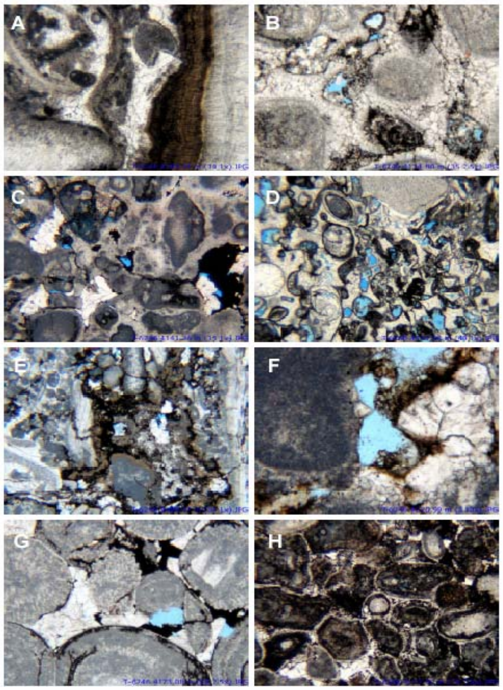

**(A) Fibrous pendant cement; (B) mycrostalactitic or pendant cements; (C, D) meniscus and pendant cements, burial dissolution of interparticle porosity followed by blocky calcite cement and bitumen; (E) alveolar fabrics; (F) vadose cementation followed by dissolution of grain boundaries, blocky calcite cement and bitumen. (G, H) minor cementation and compaction leads to fitted fabrics.**

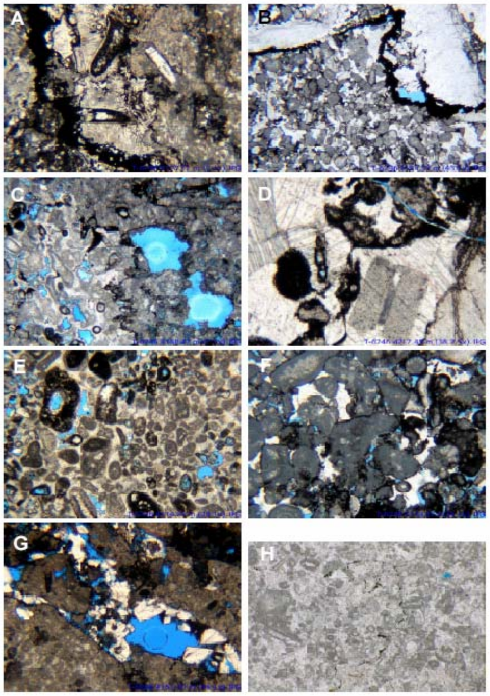

**A) Stylolite with dark brown micrite and possibly bitumen; (B, C) dissolution associated with stylolite; (D) syntaxial overgrowth cements on crinoids reduce interparticle porosity, dissolution corroded cement and grains; (E) equant to rhombic spar occludes interparticle pores; (F) corroded grains followed by blocky calcite in interparticle porosity; (G) partially open fracture occluded by blocky calcite cement and bitumen; (H) porosity filled by cement and completely recrystallized to fine calcite spar.**

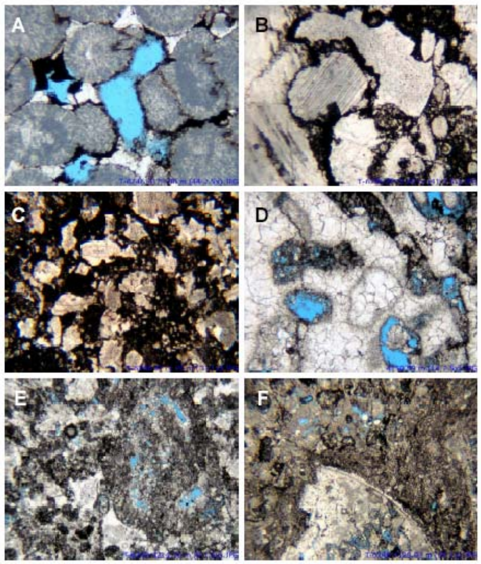

**(A) Burial (?) dissolution of interparticle pores to form vugs prior to bitumen; (B,C) corrosion of crinoids and syntaxial overgrowth cements and bitumen emplacement; (D) recrystallization following partial cementation of interparticle porosity, note early moldic porosity was occluded by blocky calcite (see micrite envelop) while a later dissolution phase generated open molds lined by bitumen. (E, F) finely recrystallized fabrics associated with intercrystalline and minor moldic porosity.**

# LATE VISEAN TO BASHKIRIAN PLATFORM CYCLICITY IN THE CENTRAL TENGIZ BUILDUP, PRICASPIAN BASIN, KAZAKHSTAN: DEPOSITIONAL EVOLUTION AND RESERVOIR DEVELOPMENT

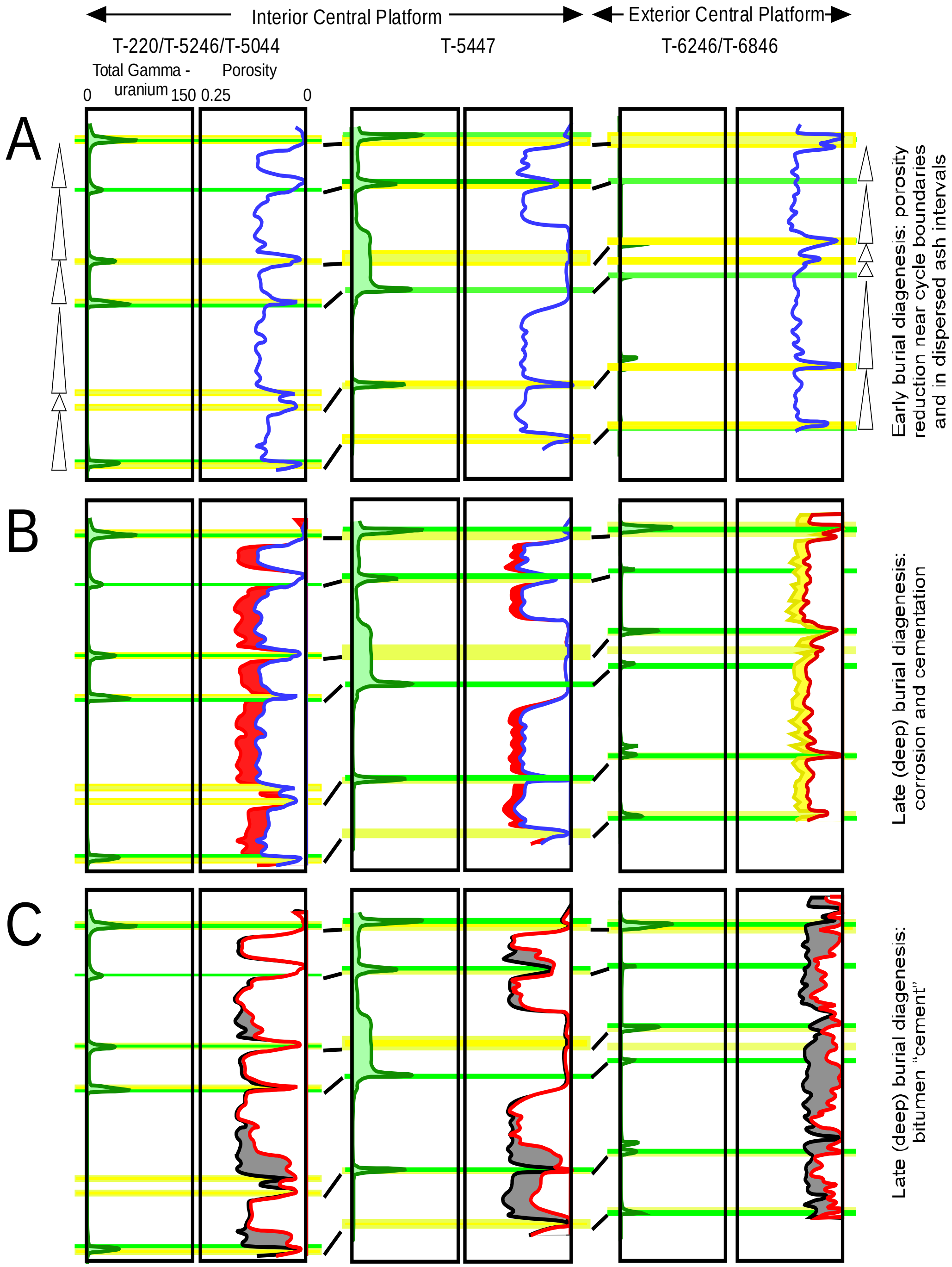


**Porosity generation and reduction events that are linked to the major diagenetic phases are indicated for a stratigraphy that includes thin low energy lagoonal intervals alternating with volcanic ash beds (yellow and green horizons) and thick intervals of high energy grainstone (white). Detailed correlation shows that lagoonal intervals and ash beds are not always associated and/or continuous between well locations, and cycles (triangles) may vary slightly in thickness over kilometers distance.**

**(A) Porosity curves with a blocky shape are the result of early burial processes including porosity loss around cycle boundaries related to the presence of thin ash beds and corrosion and cementation related to meteoric diagenesis (porosity is blue). Locally thick grainstone intervals have low porosity and show the presence of elevated levels of dispersed ash concentrated in frequent stylolites.**

**(B) Late burial events leading to corrosion, and enhanced blocky porosity curves, in interior central platform (red) and porosity reduction in the exterior central platform (yellow); alternatively, corrosion in the exterior central platform was lower compared to the interior central platform.**

**(C) Bitumen, which is emplaced during late burial, acts as "cement" and reduces porosity. Bitumen volume increases from the interior to the exterior central platform and margin and obscures correlation using the porosity curves.**

**J. A. M. Kenter** and **P. M. Harris**, Chevron Energy Technology Company
**J. F. Collins** and **L. J. Weber,** ExxonMobil Development Company
**G. Kuanysheva** and **D. J. Fischer**, TengizChevroil

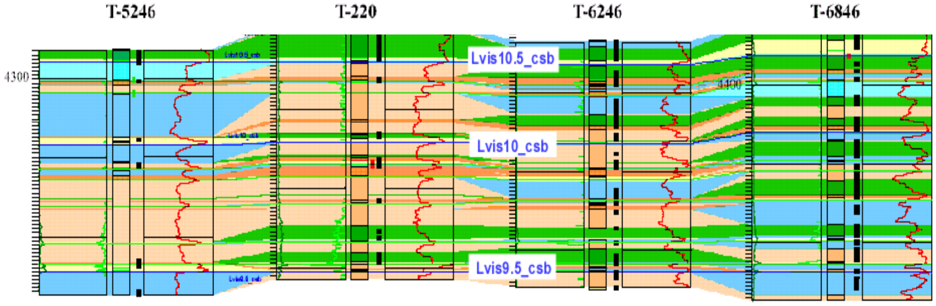


**Lateral facies and thickness continuity of the sequences between Lvis10.5_csb and Lvis9.5_csb are shown between the T-5246, T-220, T-6246 and T-6846 wells. The cyclic and blocky high-low porosity character is visible in nearly bitumen free wells (T-5246 and T-220) and represents, respectively, alternating grainy facies and lagoonal mud intervals with volcanic ash. Though the interval in T-5246 represents high energy and essentially mud free grainstone and that in T-220 is lower energy and packstone-grainstone facies, no visible difference is observed on the porosity log.**

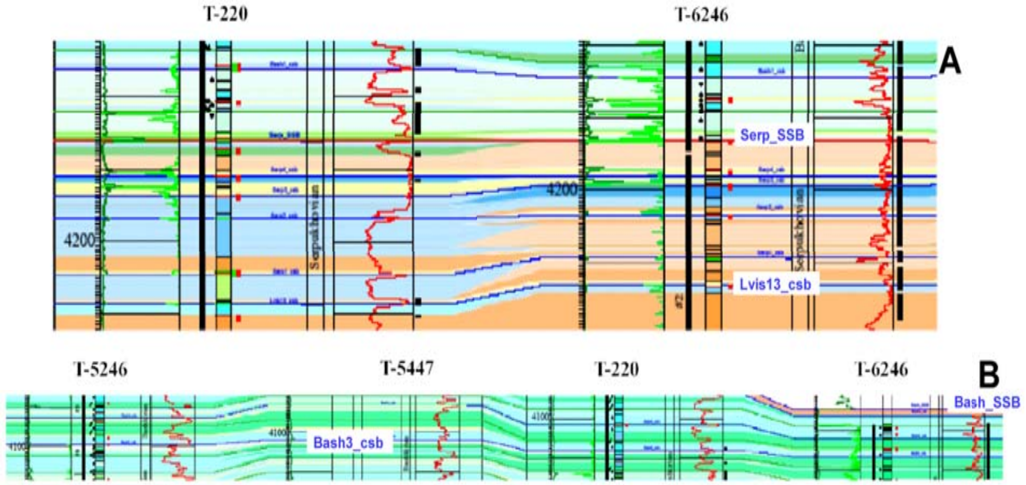


**The lateral facies and thickness continuity of sequences between the Serp_SSB and Lvis13_csb are shown for the T-220 and T-6246 wells in (A) and between the Bash3_csb to Bash4_csb for the T-5246, T-5447, T-220 and T-6246 wells in (B). The lower portion of the Bash1_csb, mostly well sorted ooid grainstone (OG), is invaded and cemented by bitumen all across the platform.**

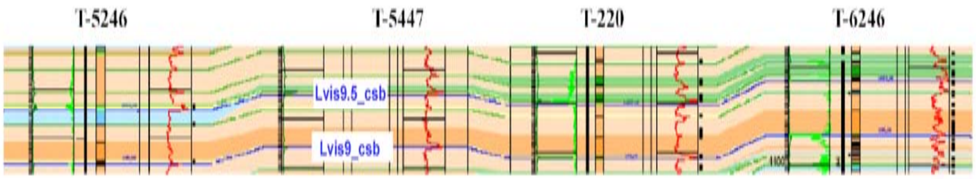


**Lateral facies and thickness continuity of sequence Lvis9.5_csb to Lvis9_csb is shown for wells T-5246, T-5447, T-220, and T-6246. Towards the southwestern (interpreted as outer platform) margin and away from the central platform to the north (T-5044), overall bitumen in the Lvis_SSB to Bash_SSB section increases (up to 2-4, % rock volume bitumen in some parts of T-6246) and generally elevated levels of bitumen are usually confined to the lower part of the cycle.**

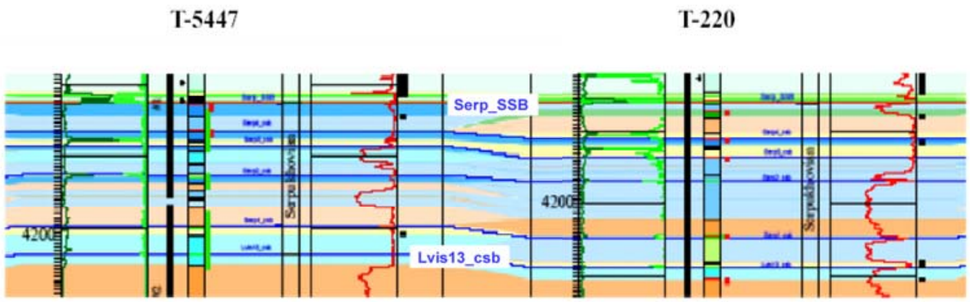


**The lateral facies and thickness continuity of sequences between Serp_SSB and Lvis13_csb is shown for wells T-5447 and T-220. In addition to bitumen reducing porosity, dispersed volcanic ash in high-energy grainstone facies locally has an even greater effect on porosity in the central platform. Volcanic ash dispersed in the SPG and CgPR lithofacies in the Serp1_csb sequence at T-5447 reduces porosity to nearly zero percent, generating a flat porosity curve, whereas the same facies interval at T-220 retained high porosity.**